

# **Wavefront Control Algorithms and Analysis for a Dense Adaptive Optics System with Segmented Primary Mirror**

Mark Milman

Amir Fijany

Jet Propulsion Laboratory  
California Institute of Technology  
4800 Oak Grove Drive  
Pasadena, CA 91109

## **ABSTRACT**

This paper presents the development and analysis of a wavefront control strategy for a dense adaptive optics system with segmented primary mirror. Systems of this type represent a substantial departure from most conventional adaptive optics systems in that the deformable element is the segmented primary mirror and the feedback signal includes both the local wavefront tilt and the relative edge mismatch between adjacent segments. One of the major challenges in designing the wavefront control system is the large number of subapertures that must be commanded. A fast and near optimal algorithm based on the local slope and edge measurements is defined for this system.

**1. Introduction.** This paper presents the development and analysis of a wavefront control scheme for a dense adaptive optics system with segmented primary mirror [1--5]. In addition to the analysis of the controller, connections with optimal controllers and previously studied heuristic controllers are established. And, perhaps most importantly, because the systems considered in [2] involve perhaps tens of thousands of subapertures we introduce "fast" algorithms that will help to make practical their implementation. These algorithms are explored more fully in the companion paper [6].

The controller studied in this paper is derived from the assumption that the wavefront is locally flat over each subaperture. This assumption leads to a strategy that involves a two-step implementation, requiring first the local correction for wavefront tilt for each subaperture, followed by a global correction for the piston error. Conventional AO systems employing a continuous deformable mirror as the correcting optical element achieve the piston correction via a wavefront reconstruction process based on local gradient (tilt) information. The reconstruction process leads to a discretized Poisson equation with normal boundary conditions to estimate the wavefront. Because the adaptive optical element for this system is not a continuous surface, a slightly different path must be taken to correct the wavefront. This process entails the use of edge displacement measurements between adjacent mirror segments to supplement the tilt measurements to fill in the gaps, so to speak, created by the discontinuous surface. The wavefront control law based on this formulation is shown to lead to a discretized Poisson equation as well. The derived control law turns out to be identical to a control strategy based on the heuristic of first correcting for local tilt and then minimizing the edge mismatch error in a least squares sense to make the segmented mirror behave as a membrane, in analogy with continuous deformable mirrors. This particular strategy has been pursued in several articles for controlling segmented mirrors [1--5]. Here we offer a slightly different interpretation of this control strategy by connecting it with a global piston correction. This connection is never made explicit in these papers.

It turns out that this control law is *not* optimal. The optimal controller exploits the coupling that exists between the tilt measurement/correction and the edge measurements [7]. We define the relationship between this optimal controller and the suboptimal controller described above, and show that they are equivalent when there is no tilt measurement error. The simplicity of the structure of the suboptimal controller achieved by discarding the coupling terms is dramatic, both in terms of implementation and analysis.

Because the control law is derived from a discretized Poisson equation, we are able to establish some *a priori* error bounds. It is shown that the global rms piston error due to edge sensing is approximately of unity magnitude for very large systems consisting of the order of 105 subapertures. This result is important for setting accuracy requirements on candidate edge sensing devices. We also show that the piston error grows logarithmically with the number of subapertures. Hence, reducing segment size places tighter requirements on the edge sensor, although rather mildly. The effect of reducing segment size actually has a more substantial effect on the reconstruction error due to tilt error. This growth turns out to be linear with decreasing subaperture size if the number of sensing photons over the entire aperture is fixed.

The computational aspects of implementing a controller for very large adaptive systems is truly one of the tentpoles associated with making these systems practical. Having the control matrix "in hand" does not represent the most viable solution to this problem, since a system with  $N^2$  subapertures requires  $N^4$  flops for each correction. (For example, the SELENE system [2], which is envisioned to have approximately 250,000 subapertures, a bandwidth of 100 Hz translates to approximately 10<sup>14</sup> flops/sec.) Iterative methods such as multigrid to construct approximate controllers for trading computational accuracy with complexity have been investigated [5]. These iterative methods are generally nondeterministic in the sense that obtaining precise *a priori* error

bounds is difficult. Here we introduce a novel implementation concept that is both “fast” and deterministic by exploiting the relationship between the control law and the discretized Poisson equation. This implementation requires  $O(N^2 \log N)$  floating point operations to implement, where  $N^2$  again denotes the number of subapertures. The algorithm is based on embedding (regularizing) the Poisson problem defined over the aperture into a problem defined on a square. This approach is in spirit similar to *capacitance* methods for regularizing domains in elliptic problems [8,9]. However, the approach is unique in that we fully exploit the special structure of the least squares formulation and the availability of boundary information to extend the problem to a regular domain. (Capacitance methods are quite different as they rely on decomposing the domain into regular subdomains and matching boundary conditions between the subdomains.) Fast solvers based on the FFT (requiring just  $O(N^2 \log N)$  flops) exist for solving the Poisson problem on a square domain [9, 10]. (A more complete exposition of these algorithms is presented in [6].) Bounds on the increased covariance of the wavefront estimate introduced by the embedding procedure are also presented. These bounds indicate the increased error to be rather benign, perhaps a .13 increase for very large systems with 105 subapertures.

**2. An idealized problem.** Let  $w(x)$  denote the instantaneous wavefront, and let the segmented primary surface be represented by the piecewise linear function  $u(x)$ ,

$$u(x) = \sum_i \chi(\Delta_i)(x) u_i(x), \quad (1)$$

where  $\Delta_i$  denotes the  $i^{th}$  segment,  $\chi(\cdot)$  = characteristic function ( $\chi(\Delta_i)(x) = 1$  if  $x \in \Delta_i$ , zero otherwise), and  $u_i(x)$  is linear. Let  $x_i$  be the centroid of  $\Delta_i$ . Ideally we would like to minimize the wavefront error  $J$ ,

$$J = \int_A |w(x) - u(x)|^2 dx, \quad A = \cup \Delta_i. \quad (2)$$

From (2) we write

$$J = \sum_i \int_{\Delta_i} |w(x) - u_i(x)|^2 dx, \quad (3)$$

and note that it is sufficient to independently minimize the error for each segment.

Now given that  $u_i$  is linear, and assuming that  $w$  is  $C^2$  (two continuous derivatives), a reasonable control strategy is to choose  $u_i$  so that

$$u_i(x) = w(x_i), \quad \text{and} \quad \nabla u_i(x_i) = \nabla w(x_i). \quad (4)$$

This controller corrects for piston, tip and tilt across each subaperture. By satisfying (4) we have for  $x \in \Delta_i$ ,

$$|w(x) - u_i(x)| \leq 1/2 \max_{\xi \in \Delta_i} \langle (x - x_i), W(\xi)(x - x_i) \rangle, \quad (5)$$

where  $W(\xi)$  denotes the Hessian of  $w$ . Now if we assume that the distance between adjacent centroids is  $h$ , and the area of the total aperture is  $d^2$ , the number of segments comprising the “primary, call it  $N$  is of order  $N = O(d^2/h^2)$ . The error  $J$  in (2) is now approximated as

$$\begin{aligned} J &= \sum_i \int_{\Delta_i} |w(x) - u_i(x)|^2 dx \\ &\leq 1/2 \sum_i \max_{\xi \in \Delta_i} |W(\xi)|^2 \int_{\Delta_i} |x - x_i|^4 dx \\ &\approx d^2 O(h^4), \end{aligned} \quad (6)$$

since

$$\int_{\Delta_i} |x - x_i|^4 dx = O(h^6)$$

and  $N = O(d^2/h^2)$ . Hence, the normalized rms wavefront error is

$$\sqrt{J/d^2} = O(h^2) \quad (7)$$

where the constant is of the order  $\sup_{\xi \in \Delta} W(\xi)$ . We note that this controller essentially corrects for the piston, tip, and tilt across each subaperture. Nell [11] has derived an expression for the error as a function of the residual uncorrected Zernike terms of the disturbance, and in this case has shown the residual error to be approximately .13 radians<sup>2</sup> of phase based on a Kolmogorov turbulence spectrum.

3. The **nonidealized** problem. The idealized situation above is characterized by perfect reconstruction of the wavefront  $w(x)$  followed by the implementation of the control law defined in (4). This controller presupposes both global knowledge of the wavefront *and* of the aperture function  $u(x)$ . In actual application neither of these is available. But before considering this configuration, we will first treat an intermediate case between the ideal and actual to show how edge sensing contributes to the wavefront reconstruction problem.

The prototype segmented mirror system we study here is based on the SELENE configuration [2]. SELENE consists of hexagonal segments arranged in the figure below:

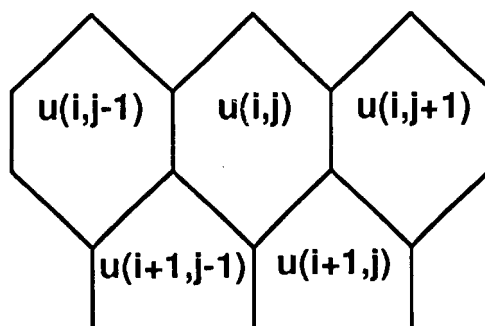


**Figure 3.1. Aperture Indexing Scheme**

We take the distance between adjacent centroids to be  $h$ . Now we make the following assumptions:

- (i)  $w(x)$  must be estimated from the wavefront tilt measurements  $\nabla w_{ij} = \nabla w(x_{ij})$ .
- (ii)  $u_{ij}$  can only be estimated from edge displacement measurements,  $\epsilon_{ij}$ , and segment tilt measurements  $\tau_{ij} = \nabla u(x_{ij})$ .

Here  $\epsilon_{ij}$  and  $\tau_{ij}$  are both 2-vectors,  $\epsilon_{ij} = [\epsilon_{ij}^x \ \epsilon_{ij}^y]$ , and  $\tau_{ij} = [\tau_{ij}^x \ \tau_{ij}^y]$ . (In the SELENE setting we only measure the difference  $\nabla w_{ij} - \tau_{ij}$ . This case will be taken up shortly.)

Let  $\hat{w}$  denote a least squares or minimum variance estimate of  $w$ . (Without loss of generality we will assume that  $\hat{w}$  has been normalized so that  $\sum_{ij} \hat{w}_{ij} = 0$ .) The geometry in the figure leads to the edge displacement relationship

$$\epsilon_{ij}^x = u_{ij+1} - u_{ij} - h/2(\tau_{ij+1}^x + \tau_{ij}^x) \quad (8)$$

for horizontal] y adjacent segments; and for diagonally adjacent segments

$$c_{ij}^y = u_{i+1j} - u_{ij} + \frac{h}{2\sqrt{2}}(\tau_{i+1j}^y + \tau_{ij}^y - (\tau_{i+1j}^x + \tau_{ij}^x)). \quad (9a)$$

Because each segment of SELENE has edge sensors on every side, there is another measurement corresponding to the southwest diagonal,

$$c_{ij}^s = u_{i+1j-1} - u_{ij} + \frac{h}{2\sqrt{2}}(\tau_{i+1j-1}^y + \tau_{ij}^y - (\tau_{i+1j-1}^x + \tau_{ij}^x)). \quad (9b)$$

(We will ignore this measurement in the analysis and algorithm development that follows, but revisit it in [6].) Introduce the difference operator  $A$ ,

$$A = \begin{bmatrix} A^x \\ A^y \end{bmatrix}, \quad (10)$$

where

$$A^x u = u_{ij+1} - u_{ij} \quad (10a)$$

and

$$A^y u = u_{i+1j} - u_{ij} \quad (10b)$$

for  $u = [u_{11} \ U_{12} \dots]$ , (i.e., stacking  $u$  by rows in the array). Then (8)-(9) can be written as

$$Au = b \quad (11)$$

where  $b$  is a linear combination of the *measured* tilts. Now let  $\hat{u}$  denote a least squares estimate (or minimum variance estimate) of  $u$ . We will assume again that  $\hat{u}$  has been normalized so that  $\sum \hat{u}_{ij} = 0$ . In this intermediate case a compensation scheme can be defined by the local tilt command,  $\Delta\tau$ ,

$$\Delta\tau = \nabla w - \tau, \quad \tau^+ = \tau + \Delta\tau \quad (12)$$

followed by the differential piston command,  $\Delta u$ ,

$$\Delta u = \hat{w} - \hat{u}, \quad \hat{u}^+ = \hat{u} + \Delta u. \quad (13)$$

Here  $\tau, \hat{u}^+$  denote the updated tilt and piston vectors. Note again that the differential command  $\Delta u$  requires the global reconstruction of the wavefront  $w$ , while  $\Delta\tau$  only requires local measurements.

Next we will treat the more general SELENE case where we do not have independent measurements of  $\nabla w$  and  $\tau$ , but only of their difference  $y$ ,

$$y_{ij} = \nabla w_{ij} - \tau_{ij}. \quad (14)$$

Note that we still have the differential tilt command via (12)

$$\Delta\tau = y, \quad (15)$$

but we cannot use (13) for the differential piston command because the estimates  $\hat{u}, \hat{w}$  cannot be formed. However, observe that to implement (13) it is only necessary to have an estimate of the *difference*  $w - u$ . To this end assume that (15) has been implemented so that we may write

$$\nabla w = \tau. \quad (16)$$

Now since

$$\tau_{ij}^x = \frac{w_{ij+1} - w_{ij}}{h} + O(h^2), \quad (17)$$

substituting (17) into (8) gives (neglecting the  $O(h^2)$  term)

$$\begin{aligned} \epsilon_{ij}^x &= u_{ij+1} - u_{ij} - \frac{h}{2} \left[ \frac{w_{ij+2} - w_{ij+1}}{h} + \frac{w_{ij+1} - w_{ij}}{h} \right] \\ &= u_{ij+1} - u_{ij} - 1/2[w_{ij+2} - w_{ij}]. \end{aligned} \quad (18)$$

Also observe that

$$\tau_{ij}^y = \frac{\sqrt{2}}{h} [w_{ij} - w_{i+1j} + \frac{h}{\sqrt{2}} \tau_{ij}^x] \quad (19)$$

since

$$w_{i+1j} = w_{ij} + \frac{h}{\sqrt{2}} (\tau_{ij}^x + \tau_{ij}^y). \quad (20)$$

Hence,

$$\tau_{ij}^y = \frac{\sqrt{2}}{h} [w_{ij} - w_{i+1j}] + \tau_{ij}^x. \quad (21)$$

And consequently,

$$\begin{aligned} \epsilon_{ij}^y &= u_{ij+1} - u_{ij} + \frac{h}{2\sqrt{2}} \left[ \frac{\sqrt{2}}{h} (w_{i+1j} - w_{i+2j} + \tau_{i+1j}^x + \frac{\sqrt{2}}{h} (w_{ij} - w_{i+1j})) \right. \\ &\quad \left. + \tau_{ij}^x - \tau_{i+1j}^x - \tau_{ij}^y \right] \\ &= u_{ij+1} - u_{ij} - 1/2[w_{i+2j} - w_{ij}]. \end{aligned} \quad (22)$$

Now,  $w_{ij+1} - w_{ij}$  and  $w_{i+1j} - w_{ij}$  are close approximations to  $1/2(w_{ij+2} - w_{ij})$  and  $1/2(w_{i+2j} - w_{ij})$ , respectively. In fact all of these quantities are just difference approximations to either  $\partial w / \partial x$  or  $\partial w / \partial y$ . The magnitude of their difference is consequently  $O(h^2)$ , with constant again of order  $\max_{\xi \in \Delta_i} |W(\xi)|$ , i.e. for example

$$|1/2(w_{i+2j} - w_{ij}) - (w_{ij+1} - w_{ij})| \leq h^2 \sup_{\xi} |W(\xi)|. \quad (23)$$

Putting (18), (22), and (23) together we get

$$\epsilon_{ij}^x = u_{ij+1} - u_{ij} - (w_{ij+1} - w_{ij}) + O(h^2) \quad (24)$$

$$\epsilon_{ij}^y = u_{i+1j} - u_{ij} - (w_{i+1j} - w_{ij}) + O(h^2). \quad (25)$$

Hence, for small  $|h|$ ,

$$\epsilon \approx A(u - w), \quad (26)$$

and the least squares (or minimum variance) estimate of  $u - w$  can be obtained directly from the edge measurements after the local tilt corrections have been made. Thus the compensation scheme becomes:

- (i) Implement the differential tilt command via (15)
- (ii) Estimate  $\hat{v}$ ,  $v = u - w$ , from (26) (more on this step in a little bit)
- (iii) Implement the differential piston command via (13)

It is worthwhile to note that this two step control law can also be interpreted as minimizing the least squares error in the adjacent edge mismatch *after* tilt correction has been made. To see this suppose the differential tilt correction has been made, and now the objective is to implement a piston command to minimize the edge error. Let  $u^0$  denote the vector of current centroid displacements. Now recall (8)-(9):

$$e_{ij}^x = u_{ij+1}^0 - u_{ij}^0 - h/2(\tau_{ij+1}^x + \tau_{ij}^x) \quad (8)$$

$$e_{ij}^y = u_{i+1j}^0 - u_{ij}^0 + \frac{h}{2\sqrt{2}}(\tau_{i+1j}^y + \tau_{ij}^y - (\tau_{i+1j}^x + \tau_{ij}^x)). \quad (9a)$$

After applying the differential command  $\Delta u$  the adjusted edge error is simply

$$+e_{ij}^x = e_{ij}^x + \Delta u_{ij+1} - \Delta u_{ij},$$

and

$$+e_{ij}^y = e_{ij}^y + \Delta u_{i+1j} - \Delta u_{ij}.$$

Minimizing the vector  $e = [e^x + e^y]$  in the least squares sense leads to the problem

$$\min_{\Delta u} |e + A\Delta u|^2,$$

which is precisely the control law defined in Steps (i)-(iii) above.

This control law is very nearly optimal if the wavefront is locally flat over each subaperture. The proof of this is sketched below. Let  $w(x)$  denote the instantaneous wavefront, and let the instantaneous segmented primary surface be represented by the piecewise linear function  $u^0(x)$ ,

$$u^0(x) = \sum_i \chi(\Delta_i)(x) u_i^0(x)$$

(cf (1)). The objective is to implement a differential command  $\Delta u(x)$  of the form

$$\Delta u(x) = \sum_i \chi(\Delta_i)(x) \Delta u_i(x)$$

with each  $\Delta u_i$  a linear function on  $A_i$  to minimize the error

$$E(J) = \int_A E|w(x) - u^0(x) + \Delta u(x)|^2 dx, \quad A = \cup \Delta_i,$$

(cf (2)). Here  $E$  denotes the expectation operator, and the requirement is that  $\Delta u$  is measurable with respect to the observed data, that is, it must be a function of the tilt and edge sensor measurements. Write  $v_i(x) = w(x) - u_i^0(x)$ ,

$$v_i(x) = \sum_{j=0}^{\infty} \alpha_{ij} T_{ij}(x),$$

where for each  $i$ ,  $\{T_{ij}\}_{j=0}^{\infty}$  is a complete orthonormal system of functions on  $A_i$  with  $T_{i0}$  = piston,  $T_{i1}$  = tip, and  $T_{i2}$  = tilt. Since  $\Delta u_i(x)$  is linear,

$$\Delta u_i(x) = u_{i0} T_{i0} + u_{i1} T_{i1} + u_{i2} T_{i2}.$$

Thus we have

$$E(J) = \sum_{i=1}^{\kappa} \sum_{j=0}^2 E|\alpha_{ij} - u_{ij}|^2 + \sum_{i=1}^{\kappa} \sum_{j=3}^{\infty} E|\alpha_{ij}|^2,$$

where  $\kappa$  denotes the number of subapertures. Let  $u$  denote the vector with components  $u_{ij}$ , and let  $\alpha$  denote the vector with components  $\alpha_{ij}$ ,  $i = 1, \dots, \kappa$ ;  $j = 0, 1, 2$ . The solution to the optimization problem is to choose  $u$  as the conditional expectation,  $\hat{\alpha}$ , of  $\alpha$  given the measurements. Assuming  $\alpha_{i0} = v(x_i)$ , and  $[\alpha_{i1} \ \alpha_{i2}] = \nabla v(x_i)$ , (this is the assumption that the wavefront is locally planar), it can be shown that  $\hat{\alpha}$  is the minimum variance solution to the problem

$$\begin{pmatrix} I & 0 \\ \Psi & A \end{pmatrix} \begin{pmatrix} \nabla v \\ v \end{pmatrix} = \begin{pmatrix} y \\ c \end{pmatrix}$$

Here  $y$  and  $c$  are the tilt and edge displacement measurements *before* correction, and  $\Psi$  is the matrix that kinematically links the tilt measurement to the edge displacements. The control strategy of first correcting for the tilt, followed by piston correction (or equivalently, minimizing the edge displacements) is the solution obtained by estimating  $\nabla v$  from the tilt measurement  $y$  alone and ignoring the edge sensor measurement altogether. The optimal (i.e., minimum variance) solution (see [7]) couples the tilt and edge sensor measurements at the considerable expense of complicating analysis and inhibiting the development of fast solution techniques. Thus we opt for the suboptimal least squares solution.

Along these same lines we note that although incorporating the data  $c^s$  from (9b) is straightforward, this too has a deleterious effect in terms of algorithm design and analysis. The next two sections describe implementation and analysis of the algorithm described in (i)–(iii) above, using the sensor data  $c^s$ . The subject of utilizing the data  $c^s$  is taken up in [6].

**4. Estimating  $u - w$ .** The implementation of the control law outlined above requires solving the least squares problem

$$\min_z |Ax - c|, \quad (27)$$

where  $A$  is the difference operator defined in (10) and  $c$  is defined in (24)–(25). On a square grid this can be accomplished via the use of fast Poisson solver techniques implemented on serial or parallel machines since (27) reduces to the discretized Neumann problem

$$A^T Ax = A^T c; \quad Ax \cdot n = c_{\text{boundary}} \quad n = \text{boundary normal}$$

Although the initial aperture geometry may not be square, with a little care the resulting least squares problem can be transformed to a square. Let  $\Omega$  denote the region occupied by the aperture, and let  $R$  denote a square region containing  $\Omega$ . Now  $A$  is trivially extended from  $\Omega$  to  $R$ . However, extending the forcing term  $c$  requires a little more consideration. In the deterministic setting there are constraints on how  $c$  extends since it is derived from a potential. Specifically, “ignoring  $O(h^2)$  terms,

$$\sum_{\text{closed contour}} c_{ij} = 0.$$

This constraint can be incorporated in the following way. Suppose we begin with a solution  $x_{\text{ext}}$  defined on  $R$ , then  $c_{\text{ext}}$  is determined from

$$c_{\text{ext}} = Ax_{\text{ext}}.$$



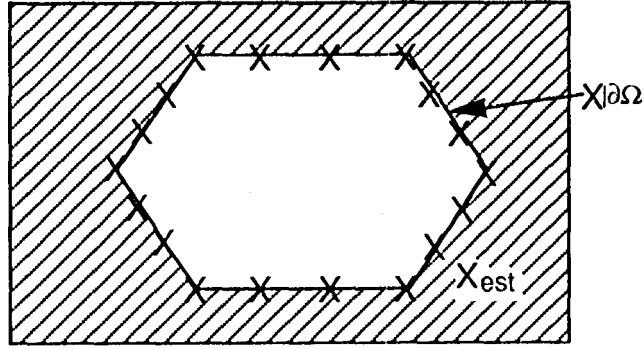


**Figure 4.1.** Regularization Embedding Scheme

Now if  $x_{ext} = x$  in  $\Omega$ , then  $c_{ext} = c$  in  $\Omega$ , and  $c_{ext}$  is an extension of  $c$  satisfying the velocity constraints. If we can determine the boundary values of  $x$  on  $\partial\Omega$ , call this function  $x|_{\partial\Omega}$ , then the potential  $x_{ext}$  can be defined arbitrarily on  $R - \Omega$ , and thereby determining an extension  $c_{ext}$  to  $c$ .

From this discussion we see that the vector field  $c$  can be extended (nonuniquely) to the square once an estimate on the boundary is obtained. This approach also works for annular regions since Hartmann sensor data is sufficient to reconstruct these boundary values as well.

To see how this is done let  $u_0, u_1, \dots, u_N$  denote the boundary values of  $x$  on  $\partial\Omega$ . The  $u_i$ 's are related by the difference equation

$$u_{i+1} = u_i + \sigma_i + \eta_i, \quad i = 0, \dots, N-1 \quad (28)$$

( $\sigma_i$  = slope measurement,  $\eta_i$  = noise) with the periodic condition

$$u_0 = u_N + \sigma_N + \eta_N \quad (29)$$

The least squares solution to this problem is obtained by solving the system

$$Ru = f, \quad f = J^T \sigma \quad (30)$$

where

$$R = \begin{pmatrix} 2 & -1 & 0 & \dots & -1 \\ -1 & 2 & -1 & \dots & 0 \\ \vdots & \vdots & \ddots & \ddots & \vdots \\ -1 & 0 & \dots & -1 & 2 \end{pmatrix}, \quad J = \begin{pmatrix} -1 & 1 & 0 & \dots & 0 \\ 0 & -1 & 0 & \dots & 0 \\ \vdots & \vdots & \ddots & \ddots & \vdots \\ 0 & 0 & \dots & -1 & 1 \end{pmatrix}$$

Now  $R$  has null space consisting of the vector  $[1 \dots 1]^T$ , corresponding to a piston. However, solutions to this problem are easily obtained by imposing a constraint on  $u$ . Once  $u$  is obtained,  $c_{ext}$  can be defined with just  $|\partial\Omega|$  (the number of points on the boundary  $\partial\Omega$ ) adds by taking  $x_{ext} = 0$  on  $R - \Omega$ , and we can proceed to solve the Poisson equation.

This embedding procedure will increase the covariance of the estimate. On an  $N \times N$  square grid, this covariance grows proportionally to  $s_N$  [12],

$$s_N = \sum_{i,j}^N \frac{1}{\lambda_{ij}}; \quad \lambda_{ij} = 4 - 2\cos\frac{\pi i}{N+1} - 2\cos\frac{\pi j}{N+1}.$$

Asymptotically,  $s_N \approx O(N^2 \log N)$ . To get a handle on how this error grows with the embedding we calculated the ratios  $s_8/s_4, s_{80}/s_{40}, s_{160}/s_{80}$ , and  $s_{320}/s_{160}$ . Each of these ratios corresponds

to the error variance increase resulting from embedding a square region into another square region of twice the size (four times the area). These results are shown below

$$s_8/s_4 = 1.1914, \quad s_{80}/s_{40} = 1.1617, \quad s_{160}/s_{80} = 1.1458, \quad s_{320}/s_{160} = 1.1309.$$

For comparison the asymptotic estimates are

$$s_8/s_4 \approx 1.5, \quad s_{80}/s_{40} \approx 1.1879, \quad s_{160}/s_{80} \approx 1.1582, \quad s_{320}/s_{160} \approx 1.1366.$$

In addition to this analytical analysis, we also did Monte Carlo simulations of the  $s_8/s_4$  case. 500 simulations were run and we empirically obtained

$$s_8/s_4 = 1.0698 \text{ (Monte Carlo).}$$

This result is slightly better than anticipated by the analytical estimate. The reason for this is that the embedding procedure *deterministically* adds data. Thus a true minimum variance estimator should very nearly yield a unity ratio for  $s_8/s_4$ . The least squares estimator is suboptimal for the embedded problem but should nevertheless produce better results than given by the analytical estimate. As another test we conducted these same simulations without properly embedding the problem. We merely extended the gradient field by using zero values outside of the  $4 \times 4$  square. The results of these Monte Carlo runs were disastrous,

$$s_8/s_4 = 1.3779 \times 10^3 \text{ (Monte Carlo, improper embedding).}$$

5. Error analysis. Let  $\hat{u}(x)$  denote the corrected primary surface. From (3) the error  $J$  is given by

$$\begin{aligned} J &= \sum_i \int_{\Delta_i} |w(x_i) - \hat{u}(x_i) + [\nabla w(x_i) - \nabla \hat{u}(x_i)](x - x_i) + \langle x - x_i, W(\xi)(x - x_i) \rangle|^2 dx \\ &= \sum_i \int_{\Delta_i} |p_i + \tau_i + q_i|^2 dx, \end{aligned}$$

where  $p_i$  denotes the piston error ( $p_i = w(x_i) - \hat{u}(x_i)$ ),  $\tau_i$  denotes the tilt error ( $\tau_i = [\nabla w(x_i) - \nabla \hat{u}(x_i)](x - x_i)$ ), and  $q_i$  denotes the quadratic remainder term. Let  $E$  denote the expectation operator. Assuming  $E(p_i) = E(\tau_i) = 0$ , and that  $q_i$  is deterministic we obtain

$$E(J) \leq \sum_i \int_{\Delta_i} [E(p_i^2) + E(\tau_i^2) + 2E(p_i^2)^{1/2}E(\tau_i^2)^{1/2} + q_i^2] dx.$$

The individual terms in the integrand above will be treated in more detail now. We first analyze the piston error

$$J_{\text{piston}} = \sum_i \int_{\Delta_i} E(p_i^2) dx.$$

Let  $v(x_i) = w(x_i) - u(x_i)$ . Recall that the control law has the form  $Au = u + \hat{v}$ . Let  $a_i^p$  denote a zero mean random variable representing the actuator piston positioning error. Then

$$p_i = v_i - \hat{v}_i + a_i^p.$$

Assuming  $a_i^p$  is independent from the reconstruction error  $v_i - \hat{v}_i$ , we have

$$E(p_i^2) = E(|v_i - \hat{v}_i|^2) + \sigma_{a^p}^2,$$

where  $\sigma_{a^p}^2$  is the variance of the actuator positioning error. Thus,

$$\sum_i \int_{\Delta_i} E(p_i^2) = \sigma_{a^p}^2 d^2 + \sum_i \int_{\Delta_i} E(|v_i - \hat{v}_i|^2) dx,$$

where  $d^2$  denotes the aperture area. The second term on the right above is the reconstruction error associated with (26). Write (26) as

$$c = Av + \eta,$$

where we assume that  $E(\eta) = 0$ , and  $E(\eta\eta^T) = \sigma_{edge}^2 I$ . Here  $\sigma_{edge}^2$  denotes the variance of the edge sensor measurement. Normalizing by the total aperture area  $d^2$  we have the mean square error

$$\begin{aligned} \frac{1}{d^2} \sum_i \int_{\Delta_i} E(|v_i - \hat{v}_i|^2) dx &= \frac{\sigma_{edge}^2 A(\Delta_i)}{d^2} \sum_i |v_i - \hat{v}_i|^2 \\ &= \frac{\sigma_{edge}^2 A(\Delta_i)}{d^2} tr(\Sigma), \end{aligned}$$

where  $A(\Delta_i)$  denotes the area of the subaperture  $\Delta_i$  and  $\Sigma$  is the covariance matrix of the estimate  $\hat{v}$ ,

$$\Sigma = E((v - \hat{v})^T (v - \hat{v})).$$

Now embed the SELFNE aperture into a square aperture with  $N \times N$  subapertures. An upper bound for  $tr(\Sigma)$  can be developed as

$$tr(\Sigma) \leq \sum_{i,j} \frac{1}{\lambda_{ij}}, \quad \lambda_{ij} = 4 \left( 2 - 2 \cos \frac{\pi i}{N+1} - 2 \cos \frac{\pi j}{N+1} \right)$$

Taking  $N = 400$ , the sum on the right above is calculated as

$$\sum_{i,j} \frac{1}{\lambda_{ij}} \approx 2.057 \times 10^5,$$

leading to an rms piston error component

$$RMS_{piston} \leq \sqrt{\frac{2.057 \times 10^5}{M} \sigma_{edge}^2},$$

where  $M$  denotes the number of subapertures.

To compute the wavefront error due to tilt error, we will assume that

$$\nabla w(x_i) - \nabla \hat{u}(x_i) = \nu_i,$$

where  $\nu_i$  is a zero mean random variable with covariance  $E(\nu_i \nu_j) = \sigma_\nu^2 \delta_{ij}$ . Note that  $\nu$  represents the combined Hartmann sensor error and tilt correction error. Thus

$$\int_{\Delta_i} E(\tau_i^2) dx = \sigma_\nu^2 \int_{\Delta_i} |x - x_i|^2 dx.$$

This integral is computed over the hexagonal region  $\Delta_i$  as

$$\int_{\Delta_i} E(\nu_i^2) dx = \frac{13}{12} \sigma_\nu^2 h^2 A(\Delta_i).$$

Thus the RMS tilt error is given as

$$RMS_{tilt} = \sqrt{\frac{13}{12}} \sigma_\nu h.$$

Combining these error components we obtain the mean square wavefront error

$$\frac{E(J)}{d^2} \leq \sigma_{ap}^2 + \frac{2.057 \times 10^5}{M} \sigma_{edge}^2 + \frac{13}{12} \sigma_\nu^2 h^2 + 2 \sigma_\nu h \sqrt{\frac{13}{12} (\sigma_{ap}^2 + \frac{2.057 \times 10^5}{M} \sigma_{edge}^2)} + \text{fitting error}.$$

If we shrink the size of the segments so that  $h \rightarrow 0$ , we observe that  $N$  grows linearly with  $h$ . And hence because of the asymptotic relationship

$$\sum_{ij}^N \frac{1}{\lambda_{ij}} = O(N^2 \log N),$$

the rms piston error will grow as  $\sqrt{\log N}$ . Thus the improvement needed in the edge sensors to maintain the same error is rather benign. On the other hand if Hartmann sensors are used for the tilt measurement, the error in this measurement is linearly related to the reciprocal of the segment size. To see this observe first that for  $h < r_0$ ,  $\sigma_\nu = 3\pi\lambda/16h\sqrt{N_{photons}}$ , where  $\lambda$  = wavelength, and  $N_{photons}$  = number of photons captured over the subaperture<sup>5</sup>. Now  $N_{photons}$  is proportional to  $h^2$ . Thus  $\sigma_\nu$  is proportional to  $1/h$ .

## ACKNOWLEDGEMENTS

The research described in this paper was carried out by the Jet Propulsion Laboratory, California Institute of Technology, under a contract with the National Aeronautics and Space Administration.

## REFERENCES

- [1] R. Ulich and J. D. G. Rather, innovative approach to next generation telescope design, SPIE Conf. 1236, Tuscon, AZ, 1990.
- [2] J. D. G. Rather, Power beaming research at NASA, SPIE OE/LASE Conf. 1628-28, Los Angeles, CA, Jan., 1992.
- [3] A. D. Gleckler, D. J. Markason, G. H. Ames, PAMELA: Control of a segmented mirror via wavefront tilt and segmented piston sensing, in Active and Adaptive Optical Components, SPIE Proc. Vol 1543, pp. 176-189, 1991.
- [4] S. Enguehard and B. Hatfield, An exact solution to segmented mirror adaptive optics control. J. Opt. Soc. Am. A, Vol. 11, pp. 874-879, Feb., 1994.
- [5] A. Lazzarini, G. H. Ames, and E. Conklin, Methods of hierarchical control for a segmented active mirror, SPIE Proc. Vol. 2121, pp. 147-158,

- [6] A. Fijany and M. Milman, Massively parallel algorithms for real-time wavefront control of a dense adaptive optics system, J. Opt. Soc. Am. A (submitted).
- [7] D. Redding, Beam transmission optical system: Analysis overview, in Proceedings of Space Laser Energy (SELENE) Wavefront Sensing and Control Workshop, Jet Propulsion Laboratory, Pasadena, CA, Feb., 1992,
- [8] E. Angel, A building block technique of elliptic boundary value problems over irregular domains, J. Math Anal. Appl., Vol. 26, pp. 75-81, 1969.
- [9] B. Buzbee, G. Golub, and C. Nielson, On direct methods for solving Poisson's equations, SIAM J. Numer. Anal., Vol. 7, pp. 627--656, 1970.
- [10] G. Strang, "Introduction to Applied Mathematics", Wellesley- Cambridge Press, Wellesley, MA, 1986.
- [11] R. J. Nell, Zernike polynomials and atmospheric turbulence, J. Opt. Soc. Am., 66, 1976, pp. 207-211.
- [12] M. Milman, D. Redding, and L. Needels, An analysis of curvature sensing methods for large aperture adaptive optics systems, J. Opt. Soc. Am. A (submitted)..
- [13] G. A. Tyler and D. L. Fried, Image position error associated with a quadrant detector, J. Opt. Soc. Am., 72, 1982, pp. 804-808.